

# Molecular dimensions in the $\delta$ and $\gamma$ phases of syndiotactic polystyrene, using small angle neutron scattering

Stéphane Moyses<sup>1</sup>, Stephen J. Spells\*

Materials Research Institute, Sheffield Hallam University, City Campus, Sheffield S1 1WB, UK

Received 8 June 1998; accepted 14 July 1998

## Abstract

The  $\delta$  phase of syndiotactic polystyrene/ethylbenzene has previously been shown to involve a sheet-like arrangement of crystal stems, with superfolding at higher molecular weights. SANS measurements have been made using tilted samples in order to separate in-plane and out-of-plane radii of gyration. Use of intensities from the whole area of the detector allows the determination of these quantities with good precision. Comparison between the out-of-plane radius and the long spacing determined from small angle X-ray measurements shows close agreement for the lower molecular weight ( $\bar{M}_w = 42\,700$ ) in both  $\delta$  and  $\gamma$  phases, while  $R_z$  is a factor of 2 larger for the higher molecular weight ( $\bar{M}_w = 124\,500$ ). This indicates that each molecule occupies a single lamella at the lower molecular weight and, on average, two lamellae at the higher one, in both  $\delta$  and  $\gamma$  phases. This provides clear evidence of tie molecules at the higher molecular weight, and also implies that the  $\delta$  to  $\gamma$  phase transition only involves a reorganisation of chain segments within those lamellae which originally contained the molecule. © 1999 Elsevier Science Ltd. All rights reserved.

**Keywords:** Syndiotactic polystyrene; Complex; Neutron scattering

## 1. Introduction

A full description of the molecular path within chain-folded polymer crystals requires the determination of: (i) any preferred fold direction; and (ii) the probabilities of folds connecting stems (the individual molecular traverses of the crystal) with all possible separations. In addition (iii) the trajectories of the folds themselves; (iv) the probabilities of cilia in the interlamellar regions; and (v) the characteristics of tie molecules linking lamellae would need to be determined.

While morphological arguments can resolve point (i) and the question of stem adjacency (point (ii)) can be addressed both theoretically [1,2], as well as by neutron scattering measurements [3,4] or infra-red (i.r.) spectroscopy [5], the quantification of points (iii)–(v) has proved more difficult. The presence of tie molecules, important in determining mechanical properties, has been investigated by several techniques, including i.r. and Raman spectroscopy [6,7]. However, these and other methods are subject to major restrictions and approximations in their quantitative use.

The measurements of molecular dimensions, presented here for a suitable polymer morphology, include data for the molecular extension in the lamellar normal direction. This provides direct evidence for the number of lamellae traversed by molecules, and hence for the presence or absence of tie molecules.

The small angle neutron scattering (SANS) method used here [8,9] makes use of the full data set available from the area detector, in order to obtain radii of gyration both in the plane of lamellae ( $R_{xy}$ ) and in the lamellar normal direction ( $R_z$ ). While more comprehensive analytical methods have since been developed [10], that used here has the advantage of allowing the key quantities, namely the radius of gyration components, to be obtained simply.

In previous papers [11–13], the structure of the syndiotactic polystyrene (sPS)/ethylbenzene system has been studied, using a range of experimental techniques. In particular, neutron scattering data for small and intermediate angles (SANS and IANS) have been used to demonstrate the sheet-like arrangement of crystal stems in the  $\delta$  phase structure, with superfolding at higher molecular weights. A high degree of adjacency of folding was required for an acceptable fit to IANS data, with folding in the crystallographic  $a$  direction implying a regular alternation of chain helicity. Investigation of the  $\delta$  to  $\gamma$  phase transition showed

\* Corresponding author. Tel.: +44-114-2253428; Fax: +44-114-2253066.

<sup>1</sup> Present address: Physics Department, Tulane University, New Orleans, LA 70118, USA.

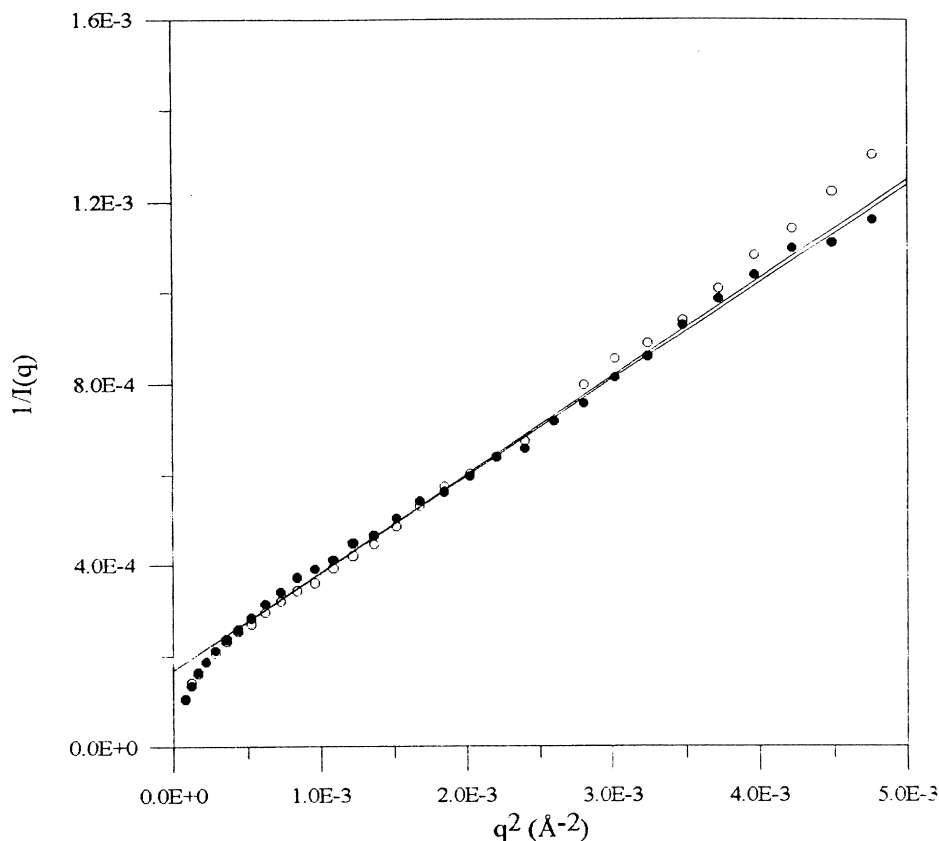


Fig. 1. Typical Zimm plots for sample SD3/2H in the  $\delta$  phase, for the intensity along the meridian ● and the equator ○ of the detector, with corresponding linear fits. The intercept at  $q = 0$  was imposed as a constant.

that decomplexation was accompanied by a temporary disordering of the helical chain segments and an increase in lamellar thickness. A molecular mechanism was proposed for the transition, with the disordering of helices facilitating the lateral movement of chain segments away from the sheets of stems. This would result in a  $\gamma$  phase structure of somewhat disordered sheets, as indicated by both SANS and IANS data.

Samples of sPS in the  $\delta$  phase were prepared by crystallisation from dilute solution in ethylbenzene, yielding well oriented mats containing around 14% of solvent. The neutron scattering measurements discussed above were all undertaken with the mat normal parallel to the incident beam. Data analysis and comparison with the results of computer simulations were essentially carried out using two-dimensional projections of the crystal stems, as is appropriate for a well oriented sample in this geometry. However, to obtain a more complete understanding of the structures and of the conformational changes at the transition, it is necessary to invoke the full three-dimensional chain trajectory. We have made SANS measurements of oriented sPS mats, with the mat normals tilted away from the incident beam. Analysis of the resultant anisotropic signal [8,9] yields radii of gyration both in the plane of the lamellae ( $R_{xy}$ ) and along the lamellar normals ( $R_z$ ). A

comparison between values obtained for  $R_z$  and for the X-ray long spacing ( $l_x$ ) then allows conclusions to be made about whether a molecule occupies one or more lamellae. This feature has important implications for the extent of molecular mobility required to accomplish the  $\delta$  to  $\gamma$  phase transition.

## 2. Experimental

Samples of sPS and fully deuterated sPS were kindly supplied by Professor V. Vittoria (Universita di Salerno) and Dr. J.-M. Guenet (Université Louis Pasteur, Strasbourg). NMR measurements showed tacticities in excess of 99%. GPC measurements were performed by RAPRA Technology Ltd (Shawbury, UK) and the deuterated materials used for this work had molecular weights ( $\bar{M}_w$ ) of 42 700 and 124 000 (samples AD and DD, respectively), with polydispersities between 2 and 3. The matrix molecular weights were 85 400 and 55 700 (samples AH and BH, respectively).

Samples containing 5% deuterated polymer were dissolved by heating to give 0.1% w/w solutions in ethylbenzene. These were transferred to a constant temperature bath for crystallisation at  $40 \pm 0.5^\circ\text{C}$  for 24 h. Samples were filtered and allowed to dry in air, as described previously

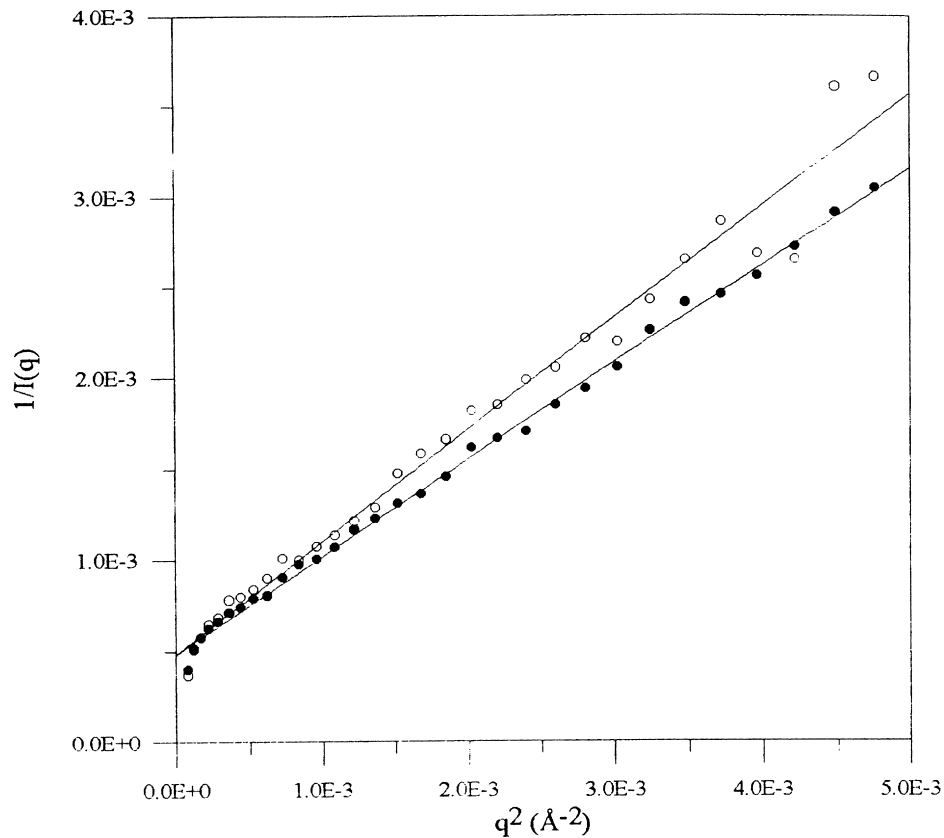


Fig. 2. Typical Zimm plots for sample 2D/1H in the  $\gamma$  phase, for the intensity along the meridian  $\bullet$  and the equator  $\circ$  of the detector. The intercept at  $q = 0$  was imposed as a constant.

[11].  $\gamma$  Phase samples were prepared by heating  $\delta$  samples at  $135^\circ\text{C}$  for 5 h.

Neutron scattering measurements were made using instrument LOQ at the ISIS neutron source. The range of scattering wavevector,  $q$  ( $= 4\pi \sin \theta/\lambda$ , where  $2\theta$  is the scattering angle and  $\lambda$  the neutron wavelength) was from  $9 \times 10^{-3} \text{ \AA}^{-1}$  to  $0.25 \text{ \AA}^{-1}$ . Samples were in the form of  $10 \times 10 \text{ mm}$  squares, stacked together and wrapped in

aluminium foil. These were held in cadmium holders with apertures of 8 mm diameter defining the beam size. A goniometer mounting was used to tilt samples by  $30^\circ$  with respect to the beam direction, about a horizontal axis.

Data reduction and analysis was mostly undertaken using the Collette program at ISIS. SANS measurements on the same samples, with the usual arrangement of the mat normal parallel to the beam direction, have already been reported

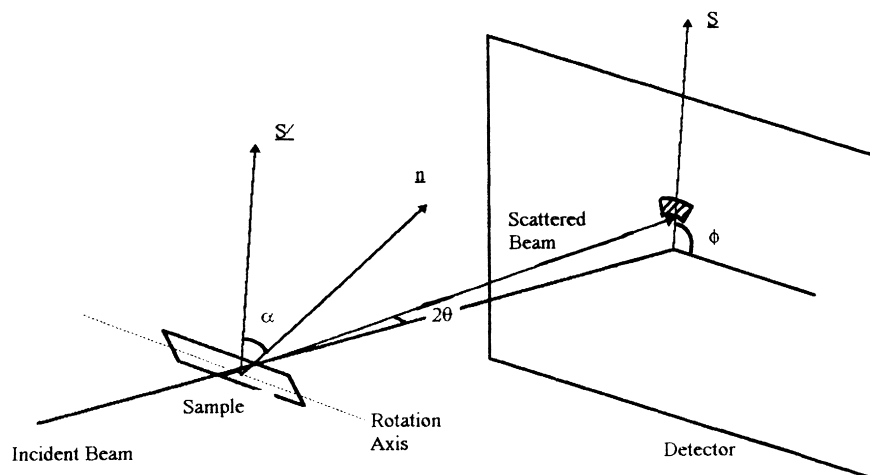


Fig. 3. Schematic diagram of the neutron scattering experiment.  $\underline{z}$  is the direction within the detector along which measurements of intensity are made and  $\underline{z}'$  passes through the sample, parallel to  $\underline{z}$ . The sample normal is  $\underline{n}$ , and the angle  $\alpha$  is that between  $\underline{n}$  and  $\underline{z}'$ .

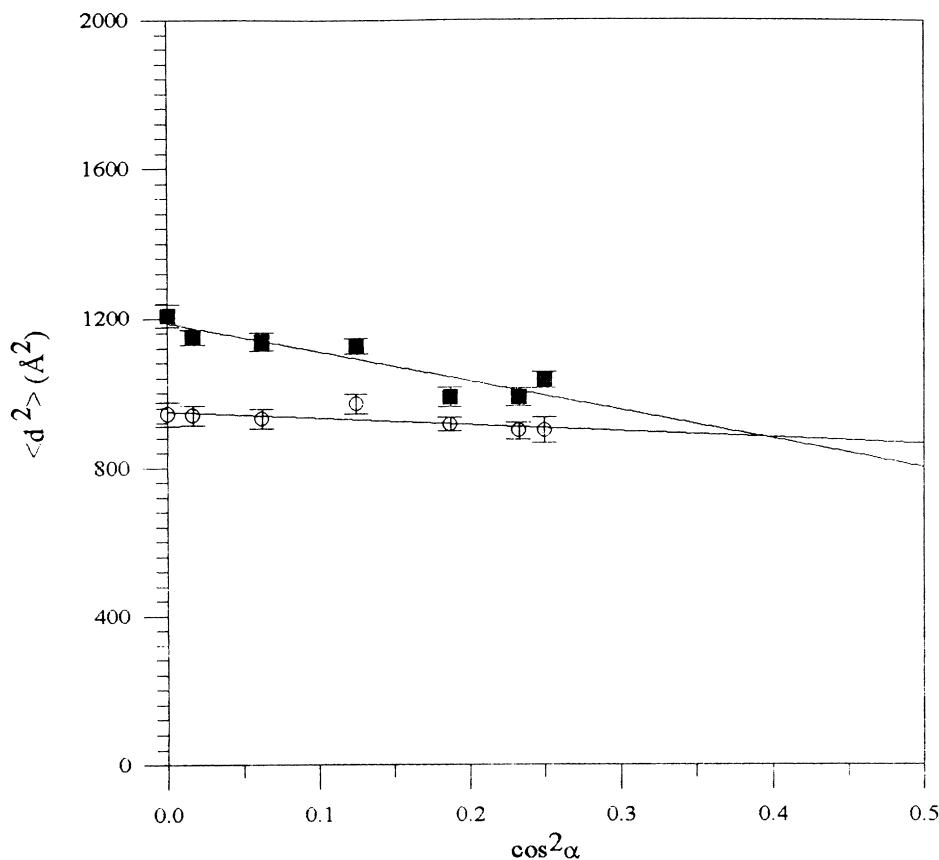


Fig. 4. Plot of  $\langle d^2 \rangle$  vs  $\cos^2 \alpha$  for sample with low molecular weight. ■:  $\gamma$  phase; ○:  $\delta$  phase.

[11] and a similar data reduction procedure was followed here. The major difference was that the detector was divided into 24 sectors, each with an azimuthal width of  $15^\circ$ . Subtraction of a purely hydrogenous sample was carried out as previously described, and the same sample was used to calibrate the intensity scale.

### 3. Results

Figures 1 and 2 show representative Zimm plots for  $\delta$  and  $\gamma$  phase samples, respectively, using data for equatorial and meridional sectors in each case. As with previous isotropic data, the plots show small excess intensity at the smallest angles, with linear behaviour well within the limit of  $q < 1/R_g$ . Fits were obtained, using the requirement that for all sectors the same intercept is obtained at  $q = 0$ . The data for each sector can be represented by:

$$\frac{I(0)}{I(q)} = 1 + q^2 \langle d^2 \rangle \quad (1)$$

where  $d$  is the distance of part of the molecule from its centre of gravity, projected onto the direction ( $\underline{S}'$ ) through the sample which is parallel to the direction in the plane of the detector ( $\underline{S}$ ) along which the intensity is measured [9]. An angle  $\alpha$  is then defined as the angle between the measurement direction ( $\underline{S}$ ) and the sample normal ( $\underline{n}$ ) (see Fig. 3).

Following reference [9], the behaviour as a function of the angle  $\alpha$  can be written:

$$\langle d^2 \rangle = \langle a \rangle + \langle b \rangle \cos^2 \alpha \quad (2)$$

where

$$\langle z^2 \rangle = \langle a \rangle + \frac{\langle b \rangle}{3} \left[ 1 + \frac{2}{\langle P_2(\gamma) \rangle} \right] \quad (3)$$

and

$$\langle l^2 \rangle = 2 \langle a \rangle + \frac{2 \langle b \rangle}{3} \left[ 1 - \frac{1}{\langle P_2(\gamma) \rangle} \right] \quad (4)$$

Here,  $P_2(\gamma) = 3 \cos^2 \gamma - 1$  is a Legendre polynomial, with  $\gamma$  the angle between  $\underline{n}$ , the sample normal and  $\underline{n}'$ , a local crystallite normal. If  $\underline{r}$  is the position of part of the molecule with respect to its centre of gravity, then  $z$  and  $l$  are the components of  $\underline{r}$  along and at right angles to  $\underline{n}'$ , respectively.

Figures 4 and 5 show plots according to Eq. (2) for low and high molecular weight samples, respectively, with both  $\delta$  and  $\gamma$  phase data points shown together. To obtain in-plane ( $R_{xy}$ ) and out-of-plane ( $R_z$ ) radii of gyration then requires the use of Eq. (3) and Eq. (4), the evaluation of  $P_2(\gamma)$  from SAXS measurements and the use of the identities:

$$R_z = \langle z^2 \rangle^{1/2} \quad (5)$$

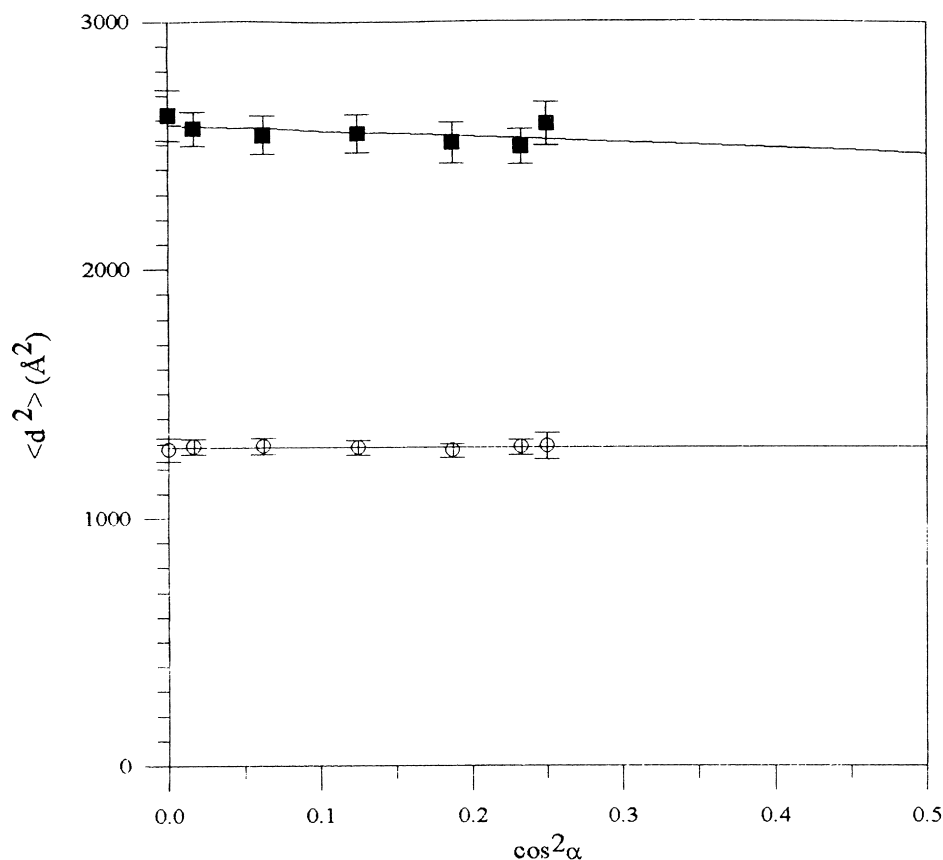


Fig. 5. Plot of  $\langle d^2 \rangle$  vs  $\cos^2 \alpha$  for sample with high molecular weight. ■:  $\gamma$  phase; ○:  $\delta$  phase.

and

$$R_{xy} = \left\langle \frac{l^2}{2} \right\rangle^{1/2} \quad (6)$$

SAXS diffraction patterns were analysed using a microdensitometer to give an average value of  $P_2(\gamma) = 0.34$  for both  $\delta$  and  $\gamma$  phases.

Values thus obtained for the radii  $R_{xy}$  and  $R_z$  are listed in Table 1, along with the quantity  $l_x/2\sqrt{3}$ , derived from the X-ray long spacing  $l_x$ . For molecules confined to a single lamella, the value of  $R_z$  is expected to equal  $l_x/2\sqrt{3}$ . As can be seen from the table, for the lower molecular weight this equality is approximated for both  $\delta$  and  $\gamma$  phase samples. However, for the higher molecular weight, values obtained for  $R_z$  are close to twice the value of  $l_x/2\sqrt{3}$  in both  $\delta$  and  $\gamma$

phases. This indicates that, on average, a molecule occupies two lamellae.

The clear implication here is that the lamellae are linked by tie molecules. In principle, knowledge of sample crystallinity should allow the number of such molecules to be determined. However, the polydispersity in this case and the resultant inhomogeneity in lamellar occupancy are too large for accurate calculations.

Also listed are the values for the radius of gyration,  $R_g$ , obtained for the oriented mats with the mat normal in the beam direction. The quantity  $R_{xy}$  is expected to be smaller by a factor of  $\sqrt{3}$ , and the data generally approximately follow this relationship.

Table 1  
Molecular dimensions

Sample	$M_w$	$R_g$ (Å)	$R_{xy}$ (Å)	$R_z$ (Å)	$l_x/2\sqrt{3}$ (Å)
DD/BH/ $\delta$	124 000	61	$36 \pm 1$	$35 \pm 2$	17
DD/BH/ $\gamma$	124 000	85	$52 \pm 2$	$45 \pm 4$	21
AD/BH/ $\delta$	42 700	52	$33 \pm 1$	$23 \pm 3$	17
AD/AH/ $\gamma$	42 700	55	$41 \pm 2$	$22 \pm 9$	21

$R_g$  is the in plane radius of gyration measured by isotropic small angle neutron scattering [11].  $R_{xy}$  and  $R_z$  are the dimensions in the mat plane and along the mat normal, respectively, as measured in this work.  $l_x$  is the long period measured by SAXS.

#### 4. Discussion

From our previous chain conformational model for the  $\delta$  phase [12], superfolding was shown to be absent at the lower molecular weight studied here, whereas a proportion of two sheet structures was found necessary to describe the higher molecular weight sample. We conclude that the probability of a molecule leaving one lamella to enter another is similar to its probability of superfolding. Considering the higher molecular weight sample, in view of the small total number of stems involved, it is likely that the two lamellae occupied

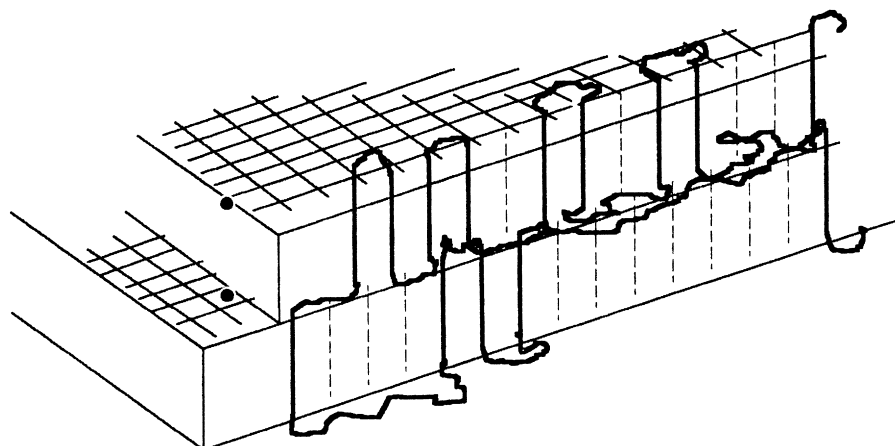


Fig. 6. Schematic diagram of the path of part of one molecule ( $\bar{M}_w = 124\,500$ ) through two adjacent lamellae. The separation of the two black dots denotes the periodicity of lamellar stacking ( $l_s$ ). The statistical arrangement of crystal stems is obtained from previous neutron scattering measurements [12].

by a single molecule are adjacent. This arrangement is shown schematically in Fig. 6.

It is worth noting that a similar model, with multiple lamellar occupation, has previously been proposed for isotactic polystyrene samples crystallised from solution at high supercoolings [14]. Features such as sheet-like growth, superfolding and the occupation of more than one lamella appear, therefore, to be general to solution crystallisation, irrespective of whether or not complex formation is involved.

The fact that the number of lamellae occupied by a single molecule remains unchanged on passing from the  $\delta$  to  $\gamma$  phase transition has significance for the mechanism of the transition. It has been shown that on heating a  $\delta$  phase sample, decomplexation involves a disordering of the helical stems [11]. We proposed that this allows lateral movement of helical segments out of (010) planes. The increase in helical order on completion of the transition is interpreted as evidence of complete stems having moved out of the original sheets, giving rise to a larger in-plane radius of gyration ( $R_{xy}$ ) in the  $\gamma$  phase (see Table 1). The present work indicates that chain mobility at the phase transition only occurs within the individual lamellae and does not involve movement into neighbouring lamellae.

### Acknowledgements

We wish to thank Dr. S.M. King (ISIS) for assistance with neutron scattering measurements.

### References

- [1] Frank FC. *Disc Faraday Soc* 1958;25:205.
- [2] Mansfield ML. *Macromolecules* 1983;16:914.
- [3] Sadler DM, Harris R. *J Polym Sci, Polym Phys Ed* 1982;20:561.
- [4] Spells SJ, Sadler DM. *Polymer* 1984;25:739.
- [5] Spells SJ, Keller A, Sadler DM. *Polymer* 1984;25:749.
- [6] Lustiger A, Ishikova N. *J Polym Sci, Polym Phys Ed* 1991;29:1047.
- [7] Egorov EA, Tshmel AE, Zhizhenkov VV. *Polymer Commun* 1998;39:497.
- [8] Sadler DM. *J Appl Cryst* 1983;16:519.
- [9] Sadler DM. *Polymer Commun* 1985;26:204.
- [10] Saraf RF. *Macromolecules* 1989;22:675.
- [11] Moyses S, Sonntag P, Spells SJ, Laveix O. *Polymer* 1998;39:3537.
- [12] Moyses S, Spells SJ. *Polymer* 1998;39:3665.
- [13] Moyses S, Spells SJ, Daniel C, Spevacek J, in preparation.
- [14] Guenet J-M, Sadler D, Spells SJ. *Polymer* 1990;31:195.